

Near-Infrared Spectrometry of Abdominal Aortic Aneurysm in the ApoE^{-/-} Mouse

Aaron Urbas, Michael W. Manning,[†] Alan Daugherty,[†] Lisa A. Cassis,[‡] and Robert A. Lodder*

Department of Chemistry, University of Kentucky, Lexington, Kentucky 40506-0055

Abdominal aortic aneurysms (AAAs) occur in 5–7% of people over age 60 in the United States. Early intervention in the disease process could have a significant impact on the incidence of complications and on patient survival, but identifying incipient aneurysms can be difficult. ApoE knockout mice develop AAAs following infusion of angiotensin II (AngII) by osmotic minipump into the subcutaneous space of mice at doses ranging from 500 to 1000 ng kg⁻¹ min⁻¹ for 7–28 days. These mice are used as models of AAA development. This study tested the hypothesis that near-IR spectrometry and PCR can determine AngII dose (SEE = 26 ng kg⁻¹ min⁻¹, SEP = 37 ng kg⁻¹ min⁻¹, r² = 0.99) and collagen/elastin (C/E) ratio (SEE = 0.38, SEP = 0.39, r² = 0.85) in mouse aortas.

A number of genetic “knockout” murine models have been developed recently to mimic human atherosclerosis¹ and abdominal aortic aneurysm² (AAA). Techniques for monitoring the onset, progression, and regression of these processes in murine models could provide valuable pathophysiological insights into the disease processes. Nondestructive in vivo techniques will be needed for proteomics studies in these models. Finally, these analytical methods may be useful in assessing the effectiveness of possible treatments.

Atherosclerosis is a chronic inflammatory process^{3–5} with complications that are the leading cause of death in western societies. Extensive research has been done to determine the complex pathophysiology of atherosclerosis, although mechanisms for various aspects are still being elucidated. Among the earliest changes in the vessel wall is an increase in retained lipoproteins,^{6–8} and subsequent oxidation,^{7,9,10} in the subendothelial matrix. Development of lipid-laden macrophages (foam cells) is

another hallmark of the early atherosclerotic process.^{11,12} Proliferation and phenotypic changes in smooth muscle cells are seen as well.^{13,14} The advanced atherosclerotic lesion may be characterized by accumulation of extracellular lipid, development of a lipid-rich necrotic core, formation of a fibrous cap, and calcification.¹⁵ Atherosclerosis in the vessel wall has been linked to aneurysm, although it is not clear that this is a causal relationship.

AAAs represent potentially life-threatening conditions that occur in up to 10% of the aged populations in industrialized nations. An aneurysm is broadly defined as a permanent localized dilatation of an artery. AAAs arise due to substantial remodeling of the extracellular matrix and are frequently accompanied by atherosclerosis. They may be manifested by catastrophic rupture, signs of pressure on other viscera, or an embolism originating in the aneurysm wall, but most are asymptomatic.

Collagen and elastin are major structural components of vessel walls that have been widely implicated in aneurysm formation, progression, and rupture. The most prevalent structural modification associated with human AAAs that has been reported is a reduction in elastin concentration in the aortic wall.^{16–22} Significant correlations between reduced elastin concentration and AAA diameter have been observed.¹⁹ Alternatively, other studies have shown that reduction in elastin concentration is essentially complete prior to dilation of AAAs.^{21,23} One proposed mechanism for reduced elastin concentrations is degradation or loss brought about by elastolysis.^{16–18,21} Other work has reported that elastin content in the vessel walls of AAAs actually increases.^{22,24} In these studies, a 2.5-fold increase in elastin content was found in AAAs versus normal aortic samples of equal length. This increase, however, was accompanied by a significantly greater increase in total matrix proteins, which suggests that reduction in elastin content is at least in part due to dilution. These results and work

* To whom correspondence should be addressed. E-mail: Lodder@uky.edu. Telephone: 859-257-9232.

[†] Present address: Department of Internal Medicine, College of Medicine, University of Kentucky Medical Center, Lexington, KY 40536.

[‡] Present address: Division of Pharmaceutical Sciences, College of Pharmacy, University of Kentucky Medical Center, Lexington, KY 40536.

(1) Glass, C. K.; Witztum, J. L. *Cell* **2001**, *104* (4), 503–16.
(2) Manning, M. W. *Vasc. Med.* **2002**, *7* (1), 45–54.
(3) Ross, R. *N. Eng. J. Med.* **1999**, *340* (2), 115–26.
(4) Ross, R. *Am. Heart J.* **1999**, *138*, S419–20.
(5) Mitchell, M. E.; Sidawy, A. N. *Semin. Vasc. Surg.* **1998**, *11* (3), 134–41.
(6) Nordestgaard, B. G.; Nielsen, L. B. *Curr. Opin. Lipidol.* **1994**, *5* (4), 252–7.
(7) Hamilton, C. A. *Pharmacol. Ther.* **1997**, *74* (1), 55–72.
(8) Williams, K. J.; Tabas, I. *Curr. Opin. Lipidol.* **1998**, *9* (5), 471–4.
(9) Navab, M. *Arterioscler. Thromb. Vasc. Biol.* **1996**, *16* (7), 831–42.
(10) Berliner, J. *Thromb. Haemost.* **1997**, *78* (1), 195–9.

(11) Navab, M. *Coron. Artery Dis.* **1994**, *5* (3), 198–204.
(12) Schwartz, C. J.; Valente, A. J.; Sprague, E. A. *Am. J. Cardiol.* **1993**, *71* (6), 9B–14B.
(13) Stary, H. C. *Eur. Heart J.* **1990**, *11* (Suppl E), 3–19.
(14) DiCorleto, P. E. *Am. J. Hypertens.* **1993**, *6* (11 Pt 2), 314S–318S.
(15) Stary, H. C. *Arterioscler. Thromb. Vasc. Biol.* **1995**, *15* (9), 1512–31.
(16) Campa, J. S.; Greenhalgh, R. M.; Powell, J. T. *Atherosclerosis* **1987**, *65* (1–2), 13–21.
(17) Powell, J.; Greenhalgh, R. M. *J. Vasc. Surg.* **1989**, *9* (2), 297–304.
(18) Rizzo, R. J. *J. Vasc. Surg.* **1989**, *10* (4), 365–73.
(19) Sakalihasan, N. *Eur. J. Vasc. Surg.* **1993**, *7* (6), 633–7.
(20) Baxter, B. T. *J. Vasc. Surg.* **1994**, *19* (5), 797–802; discussion 803.
(21) White, J. V.; Mazzocco, S. L. *Ann. N. Y. Acad. Sci.* **1996**, *800*, 97–120.
(22) Ghorpade, A.; Baxter, B. T. *Ann. N. Y. Acad. Sci.* **1996**, *800*, 138–50.
(23) White, J. V. *J. Vasc. Surg.* **1993**, *17* (2), 371–80; discussion 380–1.
(24) Minion, D. J. *J. Surg. Res.* **1994**, *57* (4), 443–6.

by others suggest that an important mechanism in AAA formation is the regulation of matrix macromolecule synthesis.^{22,24,25}

Increased collagen concentration is another matrix modification that has been widely observed in human AAAs.^{18–20,22,25} Modifications in collagen organization and deposition have been correlated to rupture in human AAAs.^{17,19,21,26} Although there are noticeable differences in the findings of these studies, it is evident that increases in the collagen-to-elastin ratio are a general observation in AAAs.

Diffuse reflection near-infrared (near-IR) spectroscopy has proven to be a useful technique for identifying chemical content of biological tissues.²⁷ Biological applications of near-IR spectroscopy include monitoring systemic and cerebral oxygenation and identifying plasma constituents including glucose, total protein, triglycerides, cholesterol, urea, creatinine, and uric acid.^{28–32} Our group has reported on the use of near-IR spectroscopy to classify human aortic atherosclerotic plaques and to identify cholesterol, HDL, and LDL in arterial wall samples.^{33–35}

This work describes preliminary research to determine the feasibility of using near-infrared spectroscopic methods to monitor collagen and elastin in the aortas of ApoE knockout mice with atherosclerosis and aneurysm formed from chronic infusion of the peptide angiotensin II (Ang II). The goal of this project is to eventually create a novel fiber-optic probe capable of collecting near-infrared spectra in mouse aortas *in vivo*.

EXPERIMENTAL SECTION

Mice. The animal model has been detailed elsewhere,³⁶ and only a brief description will be presented here. Infusion of Ang II into mature apolipoprotein E-deficient (apoE^{-/-}) mice promotes an increase in the severity of aortic atherosclerotic lesions and the formation of abdominal aortic aneurysms. The formation of aneurysms in the animal model is independent of arterial blood pressure and lipoprotein profiles; however, it requires the hyperlipidemic background and is dependent on Ang II dose and gender (males develop aneurysms at a greater incidence than females). Female apoE^{-/-} mice (back-crossed 10× into the C57BL/6J background) were obtained from The Jackson Laboratories (Bar Harbor, ME). All mice were maintained under barrier conditions. Water and normal laboratory diet were available *ad libitum*. All procedures involving animals were approved by the Animal Care and Use Committee at the University of Kentucky.

Ang II Infusion. Alzet osmotic minipumps (model 2004; Al Scientific Products, Mountain View, CA) were implanted into apoE^{-/-} mice ($n = 6$) at 6 months of age. Pumps were filled either with saline vehicle (control group, $n = 2$) or with solutions of Ang II (Sigma Chemical Co., St. Louis, MO) that delivered (subcutaneously) either 500 (medium-dose group, $n = 1$) or 1000

(high-dose group, $n = 3$) ng kg⁻¹ min⁻¹ Ang II for 28 days. At this point, the aortas were removed and analyzed.

Tissue Preparation. Aortic tissue was removed from the ascending aorta to the ileal bifurcation and placed in 4% paraformaldehyde in PBS overnight at room temperature. The intimal surface was exposed by a longitudinal cut through the inner curvature down the whole length of the aortic tree. Each aortic sample was cut into 6 roughly equal sections resulting in 36 total samples.

Instrumentation and Spectra Collection. Reference spectra of collagens I, II, III, and IV and elastin (Sigma) were obtained using a scanning monochromator system (Bran+Luebbe, Elmsford, NY) (see Figure 1 and Figure 2). Collagens I and III are the principal collagen components of the aorta. Near-IR spectra of the aorta samples were collected with a modified filter photometer system sometimes used as a high-intensity light source for near-IR arterial catheters (Bran+Luebbe). Each sample was placed on an ordinary microscope slide for analysis. The samples were not immersed in solution during spectra collection. The instrumental configuration allowed the entire tissue sample to contribute to the near-IR signal. Near-IR reflectance measurements were made at 20 wavelengths between 1445 and 2350 nm. A cubic spline-fitting algorithm (Speakeasy Computing Corp., Chicago, IL) obtained continuous spectra from the absorbance values. The spectral data were scatter-corrected prior to data analysis. Spectra from a control and a high-dose tissue sample are presented in Figure 3 for comparison. The chemical composition of the tissue samples between groups is similar, and as a result, the gross appearances of the two spectra are similar.

Collagen-to-elastin ratios for tissue samples were obtained by scanning electron microscopy (SEM) by Industrial Analytical Services Inc. (Leominster, MA) and morphometry. Detailed information on this technique can be found in the literature.^{37,38} To determine collagen-to-elastin ratios, three SEM images were obtained for each sample corresponding to the inner and outer membranes and a cross section of the aortic wall.

Data Analysis. Analytical software was written in Mathematica 4.1 (Wolfram Research, Inc.). Principal component analysis (PCA) and principal component regression (PCR) were used to analyze the data.^{39,40}

PCR was used to construct calibration models to predict Ang II dose from spectra of the aortas. A cross-validation routine was used with near-IR spectra to assess the statistical significance of the prediction of Ang II dose and collagen/elastin in mice aortas. The accuracy of the PCR method in predicting Ang II dose from near-IR spectra was determined by the *F* test and the standard error of performance (SEP) calculated from the validation samples.

RESULTS AND DISCUSSION

The spectra were investigated first by PCA to examine the relationships between the samples. The first two PCs accounted for ~89% of the variation in the data set (see Figure 4). The spectral separation among the different groups (related to Ang II

(25) Halloran, B. G.; Baxter, B. T. *Semin. Vasc. Surg.* **1995**, *8* (2), 85–92.

(26) Menashi, S. J. *Vasc. Surg.* **1987**, *6* (6), 578–82.

(27) Dempsey, R. J. *Appl. Spectrosc.* **1996**, *50*, 18A–34A.

(28) Spielman, A. J. *Brain Res.* **2000**, *866* (1–2), 313–25.

(29) Shaw, R. A. *J. Inorg. Biochem.* **2000**, *79* (1–4), 285–93.

(30) McKinley, B. A. *J. Trauma* **2000**, *48* (4), 637–42.

(31) Gabriely, I. *Diabetes Care* **1999**, *22* (12), 2026–32.

(32) Jaross, W. *Atherosclerosis* **1999**, *147* (2), 327–37.

(33) Cassis, L. A.; Lodder, R. A. *Anal. Chem.* **1993**, *65* (9), 1247–56.

(34) Dempsey, R. J. *Ann. N. Y. Acad. Sci.* **1997**, *820*, 149–69.

(35) Moreno, P. R. *Circulation* **2002**, *105* (8), 923–7.

(36) Daugherty, A.; Manning, M. W.; Cassis, L. A. *J. Clin. Invest.* **2000**, *105* (11), 1605–12.

(37) Bullivant, S. Freeze Etching and Fracturing. In *Some Biological Techniques in Electron Microscopy*; Parsons, D. F., Ed.; Academic Press: New York, 1970; pp 123–146.

(38) Sharifi, A. M. *J. Hypertens.* **1998**, *16* (4), 457–66.

(39) Thomas, E. V.; Haaland, A. C. *Anal. Chem.* **1990**, *62*, 1091–1099.

(40) Beebe, K. R.; Kowalski, B. R. *Anal. Chem.* **1987**, *59*, 1007A–1017A.

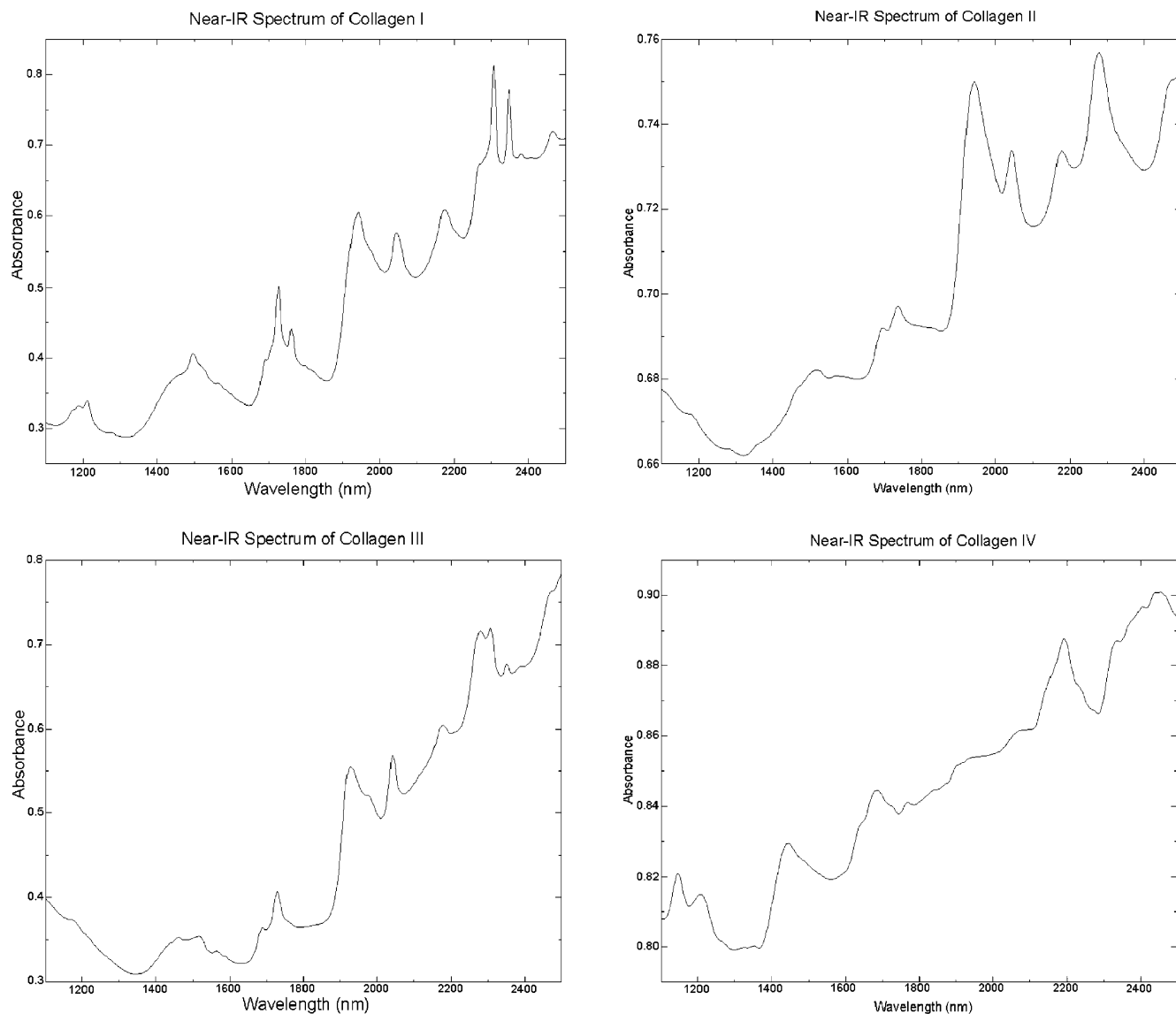


Figure 1. Near-IR spectra of collagen standards. Collagen I and collagen III are the principal collagens of the aorta. The spectra of the four collagens are distinctive, suggesting that simultaneous multicomponent analysis of collagens is possible.

dose) is significant. Also evident is the comparatively minor variation between spectra within each group (the scatter in each group comes from different mice and the position of the aortic section scanned). The control and high-dose groups contain two and three mice aortas, respectively. The medium-dose group contained samples from a single mouse.

The ability to predict Ang II dose from the near-IR spectra was examined using PCR. The SEP provides a global estimate of the prediction capabilities of the near-IR-PCR method. The SEP for Ang II dose depends on the number of PCs used in the model. The first two PCs provided the optimum prediction models, and the SEP for Ang II dose by PCR was $37 \text{ ng kg}^{-1} \text{ min}^{-1}$ (standard error of estimate (SEE) = $26 \text{ ng kg}^{-1} \text{ min}^{-1}$, $r^2 = 0.99$, $f_{0.01}$ significance).

Collagen-to-elastin ratios in the samples were estimated using SEM to determine whether a correlation existed between the near-IR spectra and this histological marker. The range of collagen-to-elastin ratios obtained was 1.4–4.5. A trend apparent in the data is a general increase in collagen-to-elastin ratio with increasing

Ang II infusion (SEE = 0.38, SEP = 0.39, $r^2 = 0.85$, $f_{0.05}$ significance). Comparison of these data with the near-IR spectra illustrates that the within-group variation is greater in the collagen-to-elastin ratios than in the near-IR spectra. The $r^2 = 0.84$ between the collagen-to-elastin ratio determined by SEM morphometry and the actual Ang II dose. Two factors that likely contribute to the error in collagen-to-elastin ratio are the limited scope of the SEM image sampling and the fact that collagen and elastin are not the only components contributing to the near-IR spectra. The entire aortic sample contributes to the near-IR spectra. Substantial lipid signals are observed in the spectra as well as signals from collagen and elastin. SEM sampling is limited to three SEM images from the inner and outer membranes and a single cross section of each vessel segment.

This work presents a macroscopic study of arterial changes in mice aorta by near-IR spectroscopy. Figure 1 demonstrates that collagens and elastin have very distinctive near-IR spectra. Collagens I and III are the principal collagens of the aorta. Figure 4 suggests that diffuse alterations occur in the aortic walls of Ang

Elastin

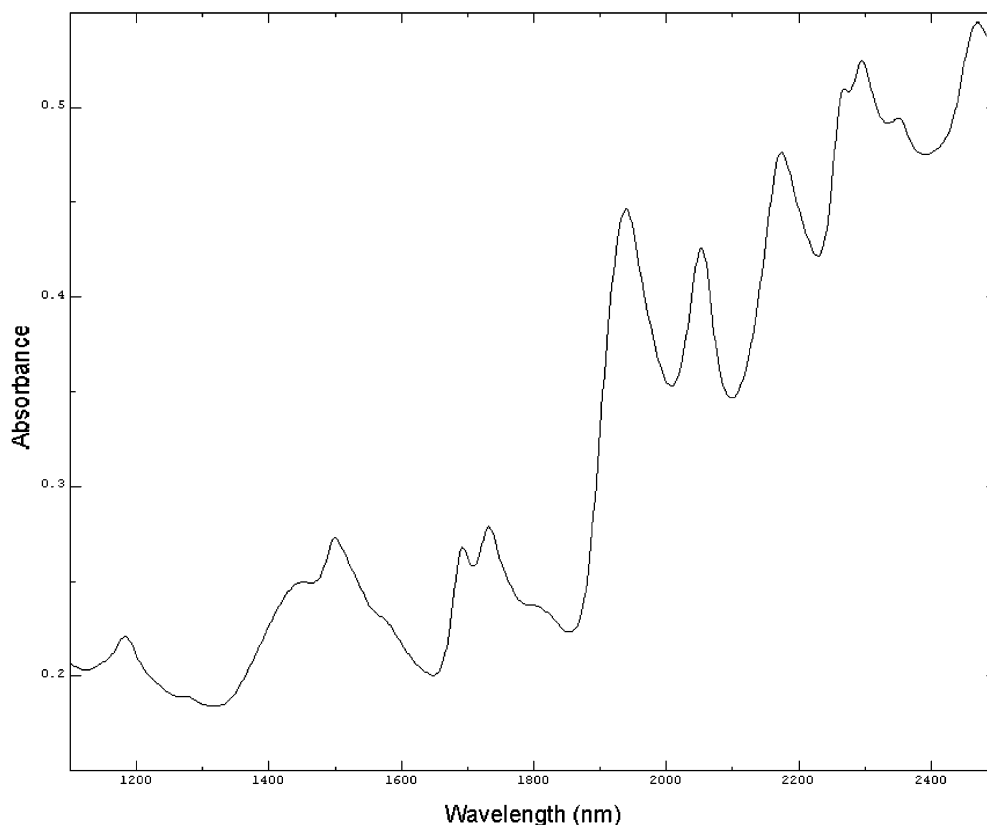


Figure 2. Near-IR spectrum of elastin standard. Elastin has a unique spectrum that differentiates it from the collagens.

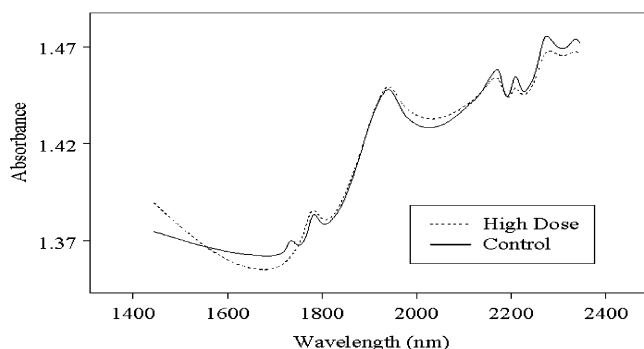


Figure 3. Examples of the near-IR spectra obtained from aorta sections of a high Ang II dose ($1000 \text{ ng kg}^{-1} \text{ min}^{-1}$) mouse and control mouse.

II-infused apoE^{-/-} mice and that these changes can be observed with near-IR spectroscopic analysis of intact tissue. The better correlation between the near-IR spectra and the Ang II dose than between the near-IR spectra and the collagen-to-elastin ratio suggests that there is more occurring in the aortas than collagen/elastin changes and that the near-IR spectra detect these additional chemical changes. This suggestion is not surprising given that near-IR spectra show contributions at some level from virtually every organic compound in any tissue. Though the data are limited, they also indicate that the near-IR identifiable characteristics of the aorta are consistent between mice within the same treatment group (this cannot be established with respect to the medium-dose group, however, because the tissue samples came from a single mouse). Together, the results support the develop-

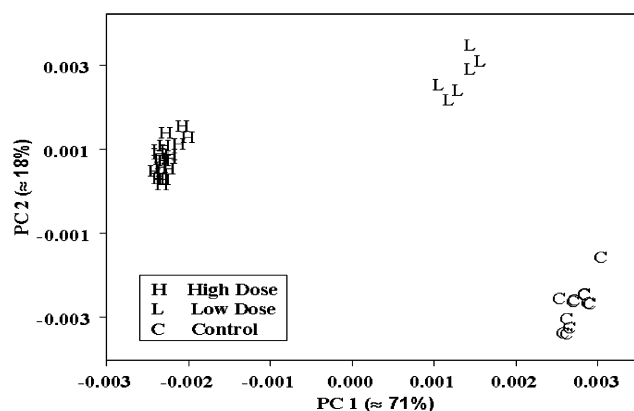


Figure 4. First two principal components of the near-IR spectra of the aorta data set. H denotes the spectra from aortic sections of the high-dose mice ($1000 \text{ ng kg}^{-1} \text{ min}^{-1}$ Ang II, $n = 18$ samples), L denotes the spectra from aortic sections of the low-dose mice ($500 \text{ ng kg}^{-1} \text{ min}^{-1}$ Ang II, $n = 6$ samples), and C denotes the spectra from aortic sections of the control mice (saline, $n = 12$ samples).

ment of a catheter and extended-use fiber-optic implant for use in the blood vessels of mice and suggest wavelengths that might be important to monitor.

In an effort to determine which spectral changes in the aortas were associated with collagens I and III and elastin composition changes, a set of sample mixtures of collagens I and III and elastin was prepared using pure lyophilized standards. Figure 5 shows the composition of each of the prepared sample standards, with the pure collagen I (C1) standard in one corner of the triangle, the pure collagen III (C3) in another corner of the triangle, and

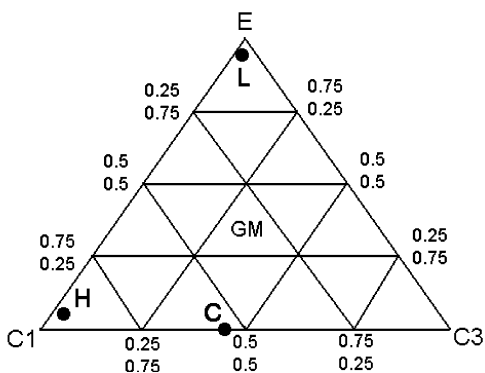


Figure 5. Diagram showing the composition of each of the prepared sample standards. The pure collagen I (C1) standard is in one corner of the triangle, the pure collagen III (C3) is in another corner of the triangle, and the pure elastin (E) in the remaining corner of the triangle. The concentrations of each of the three constituents in the standard mixtures were set at 0, 25, 50, 75, or 100% of each lyophilized protein. The vertices in the triangle represent all possible combinations of protein mixtures in the percentages given (a total of 15 mixtures including the pure corner standards). GM, the group mean, is the center of the triangle and represents a mixture of 1/3 of each protein.

finally the pure elastin in the remaining corner of the triangle. The concentrations of each constituent in the standard mixtures were set at 0, 25, 50, 75, or 100 wt % of each lyophilized protein. The vertices represent all possible combinations of mixtures in the percentages given (a total of 15 mixtures including the pure corner standards). The center (i.e., group mean, or GM in Figure 5) would represent a mixture of one-third of each protein, but this sample was not actually prepared in the set.

The reflection spectra of the 15 mixtures were compared to the reflection spectra of the 36 aorta sections by mean-centering the spectra of the mixtures and the spectra of the aortas. The difference spectra between each standard sample spectrum and the mean spectrum of the standard samples were calculated. Likewise, the difference spectra between each aorta section spectrum and the mean spectrum of the aorta sections were also calculated. The aorta difference spectra were then averaged for the control, low-dose, and high-dose Ang II groups. Finally, the difference spectra of the standards and the averaged aorta sections were then correlated using $r = \frac{\sum(s_1s_2)}{(\sum s_1^2 \sum s_2^2)^{1/2}}$, where s_1 is a spectrum 1 from the set of standards and s_2 is spectrum 2 from the set of aorta sections.⁴¹

The correlations between the average control group (saline-infused) spectrum (0 ng kg⁻¹ min⁻¹ Ang II) and each standard sample spectrum ranged between ± 0.97 . The highest correlation was with the (50, 50, 0%) (collagen I, collagen III, elastin) standard. The correlations between the average low-Ang II dose group spectrum and each standard sample spectrum ranged between ± 0.99 . The highest correlation of the average spectrum of the low-Ang II dose group was with the pure elastin (0, 0, 100%) standard. The correlations between the average high-dose group spectrum and each standard sample spectrum ranged between ± 0.87 . The highest correlation was with the pure collagen I (100, 0, 0%) standard. These high correlations suggest that much (but not all) of the variations in aorta spectra with Ang II dose can be

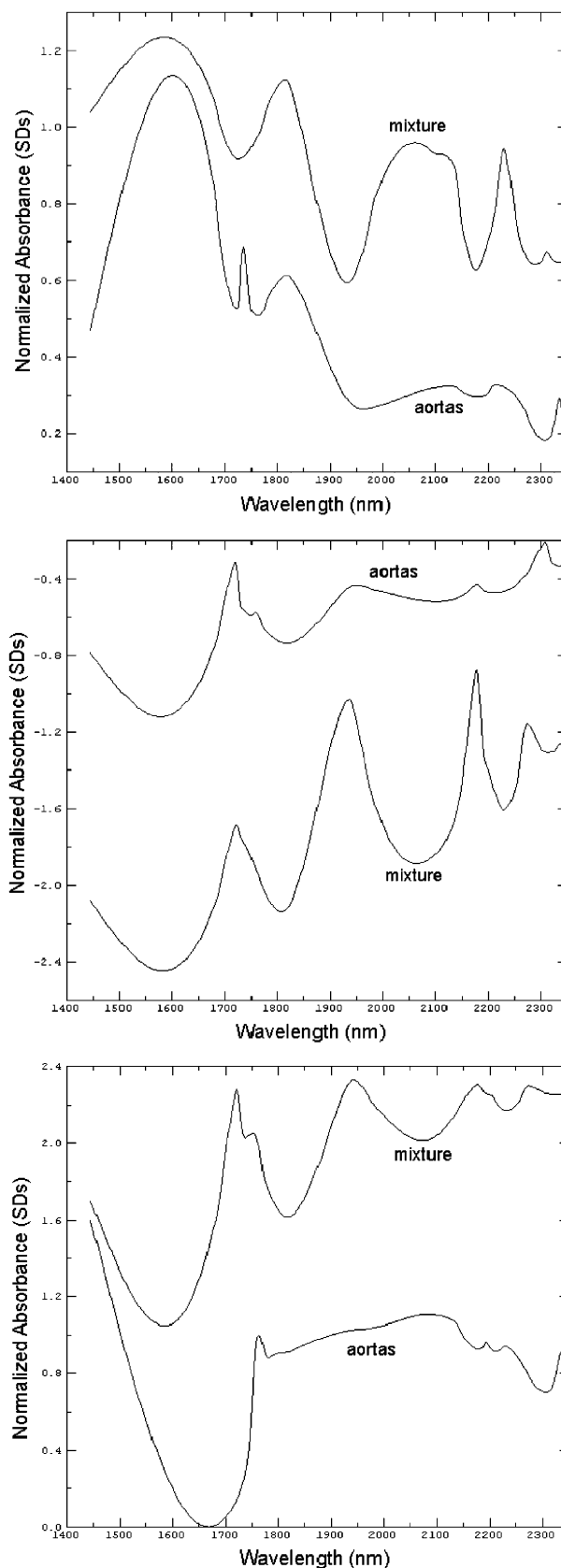


Figure 6. Spectra of the most highly correlated standard mixture of collagens and elastin and mean aorta spectrum for each treatment group: (top) control group (saline infusion); (middle) low Ang II dose, 500 ng kg⁻¹ min⁻¹ Ang II; (bottom) high Ang II dose, 1000 ng kg⁻¹ min⁻¹. The spectra in each treatment group are distinctive. The correlation between the aortic sections and the standard mixtures is highest for the control and low-dose Ang II groups.

(41) Reid, W. *Appl. Spectrosc.* **1965**, *20*, 320–325.

(42) Carney, J. M.; Landrum, W.; Mayes, L.; Zou, Y.; Lodder, R. A. *Anal. Chem.* **1993**, *65*, 1305–1313.

attributed to changes in collagen and elastin composition. The locations of the mean control (C), low-dose (L), and high-dose (H) Ang II aortic sections are shown in Figure 5. The H, L, and C points are interpolated to the location of maximum correlation to the standards. The spectra of the most highly correlated standard samples, and each treatment group is shown in Figure 6. The correlation between the aortic sections and the standard mixtures is highest for the control and low-dose Ang II groups in Figure 6. The observation that the changes in the spectra of the standard mixtures do not add up perfectly to the changes found in the aortas also suggests that there is more occurring in the aortas than collagen/elastin changes and that the near-IR spectra detect these additional chemical changes. The majority of these additional chemical changes appear to be in the C–H stretching overtone regions of the spectra (the lipid region; see Figure 3). Figure 3 shows a bathochromic shift in the C–H stretching overtones that usually corresponds to an increase in trans or saturated lipids.⁴²

This study has some limitations. The small number of mice (6) used as the source of the 36 aorta sections limits the observable variation in the data set. The lack of detailed histological data for the samples prevents the association of the spectra with specific tissue pathologies and comparison of pathology

between samples. Studies with larger, more diverse populations are necessary to better investigate the spectral trends and variation between mice.

CONCLUSIONS

Near-IR spectra are distinctive for proteins in the blood vessel wall (specifically collagens and elastin). The ability of near-IR spectrometry to collect useful spectra in aqueous environments may make it useful for proteomics in vivo. The results of this study suggest that near-IR spectroscopy is a potentially useful technique for investigating vascular changes and protein composition associated with abdominal aortic aneurysm in a mouse model of this disease. These results support an expanded study in the future to correlate near-IR spectra with chemical compositions and histological features in aortic aneurysm.

ACKNOWLEDGMENT

This work was supported in part by the American Heart Association through Grant 0151018B, the NIH through Grants HL70239 and HL55487, and the NSF through Grant CHE-9721208.

Received for review February 5, 2003. Accepted April 18, 2003.

AC034113N